ISSN: 2790-5209 DOI: 10.56028/fesr.1.3.1

# The Improved Design of a Mist Dust Removal Device for Coal Mining

Xiayi Wu*
Chongqing Vocational Institute of Engineering
*Corresponding Author e-mail: 413073992@qq.com

## Abstract

*With the development of a fully mechanized mining face, comprehensive mechanized mining face, and high-capacity and high-efficiency mining face in the coal mine, the level of mechanization and productivity is being improved, as well as dust capacity. If dust density is not reduced, it will be a hazard to the respiratory system of the miners seriously, even trigger pneumoconiosis, and the normal running of pieces of equipment will be affected, accelerating insulation equipment aging, and causing an explosion. Miners' health and safety, normal running of equipment, and economic efficiency are being injured severely.*

*Mist dust removal is the most widely used in coal mining, and it has been proven very effective. But the dust removal effect is affected because of the low interference resistance of the light control sensor, and small application scope of the solenoid valve, low agility of the spray device. In the paper, mist dust removal from coal mining was selected as the research background, and dust concentration detection and mechanism of mist dust removal were studied. The light control sensor, dust concentration sensor, and spray device were improved. By the mist dust removal device, online and real-time dust concentration monitoring can be achieved, and automatic dust removal can be realized according to the dust concentration. So, the dust concentration can be effectively reduced, working conditions can be improved, and safe production in enterprises and miners' health can be guaranteed. The main work of the paper includes the following aspects.*

*① the paper studied the application background and research actuality of dust removal at home and abroad, and analyzed the existing technology of dust removal, and pointed out the research aim and main content.*

*② to provide academic support for the improved design of a mist dust removal device, the paper analyzed dust concentration detection, mechanism of mist dust removal and main affecting factors of dust removal.*

*③ Through needs analysis, the paper presented overall architecture and functional module design.*

*④ Control module, dust concentration sensor, light control sensor, and spray device were improved. at the same time, the performance tests were also discussed.*

*⑤ the paper run the laboratory tests and field tests, the test results showed that the device can measure dust concentration truly, and realize automatic dust removal, and reduce the dust concentration effectively.*

## Keywords

*Dust hazard; Concentration detection; Mist dust removal; Device improve*

ISSN: 2790-5209 DOI: 10.56028/fesr.1.3.1

According to the demand analysis, overall structure and function design of the coal seam mining spray dust removal device, the paper improved the control module, dust concentration sensor, light control sensor, and solenoid valve and the improved performance test.

## 1. Device hardware structure

The coal seam mining spray dust removal device is composed of the control module, dust concentration sensor, light control sensor, solenoid valve, and other necessary equipment.

Considering the actual use demand and cost control factors, each control module is equipped with two dust concentration sensors, four light control sensors, and four solenoid valves during the design, which can realize four water curtain control. The electrical connection diagram of the device is shown in Figure 1.

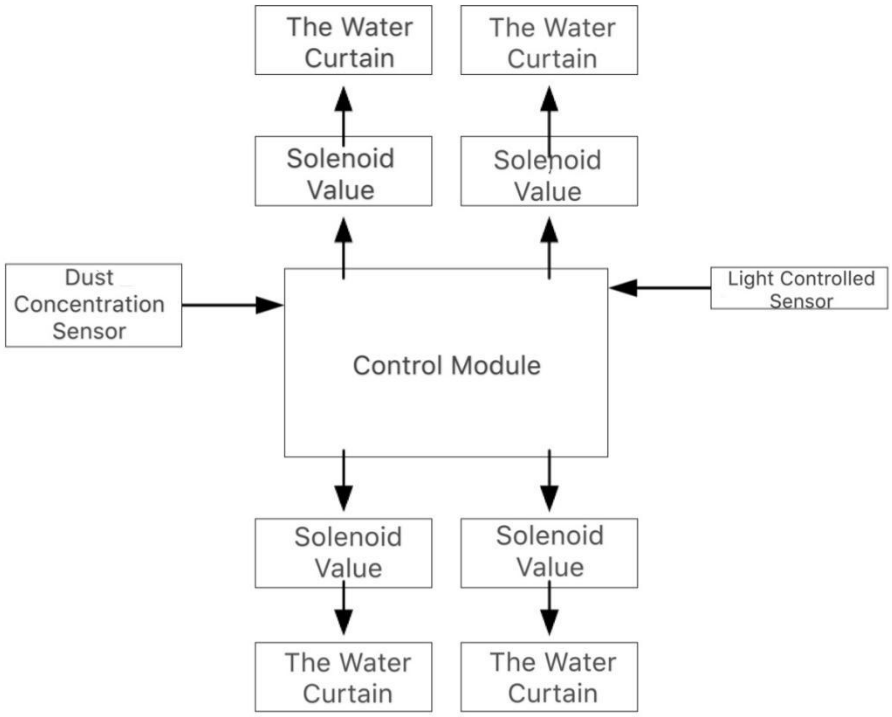


Fig. 1Sketch map of device connection

## 2. Control module

The main function of the control module is to receive dust concentration sensor signals and optical control sensor signals, and output control signals according to the actual needs. When the dust concentration exceeds the preset set value, the dust concentration sensor will send the signal to the control module, which will receive the control command to the solenoid valve, and the solenoid valve will control the spray. When someone passes by, the light sensor will convert the heat of the human body into electrical signals and send them to the control module, which will then send control instructions to the solenoid valve to control the delay spray.

The structure is shown in Figure 2.

The frequency signal output by the dust concentration sensor is isolated and sent to the microcontroller by the optical coupler, which is converted into the numerical signal by the

ISSN: 2790-5209 DOI: 10.56028/fesr.1.3.1
timing frequency counting method for data display and processing.

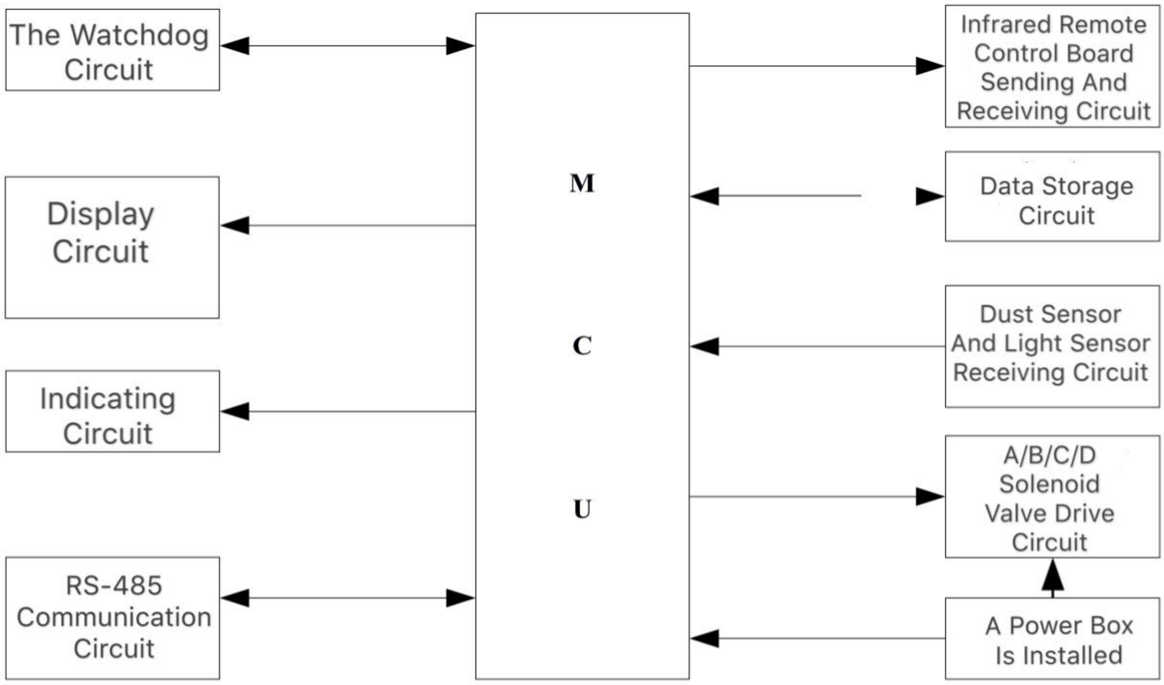


Fig. 2 Circuit structure of controls

The function of the light control sensor is to send a signal to the control module during the over-limit spray if someone passes the spray site, stop the spray, and spray again after the person passes, to avoid getting people wet.

Digital display circuit is mainly to display data and working state, by 5 ultra-bright digital tube and 74HC595 decoder, static display mode. The first digit of the five-digit display is the status indicator, and the next four digits are the data display. Because the device stores fewer data, so the data storage circuit uses 24C04, the storage capacity is 256 bytes. The sending and receiving circuit of the infrared remote-control board is mainly used to set the upper and lower limits of dust concentration, using the BL9149 chip.

The software design of the control system adopts a modular design, which is divided into a system initialization module, parameter setting module, signal sending and receiving module, control command module, interrupt module, the infrared keyboard and display module, serial communication module, and so on. The relationship between them is shown in Figure 2.1.

The main program flow of the system software is shown in Figure 2.2. After the system is started, it enters the system running state after initialization. At this time, the system detects whether there is a remote-control state key, if there is, it will execute the parameter setting program, if not, it will receive the dust sensor signal, and convert it into the dust concentration value. If the dust concentration exceeds the set upper limit, the control signal will be issued, and the solenoid valve will be opened for spray operation until the dust concentration is lower than the set value. In the process of spraying, the system begins to receive signals from the light control sensor. When someone is detected passing by, the system will issue a control signal, close the solenoid valve to stop spraying, and re-open the solenoid valve to spray when the delay time is reached.

ISSN: 2790-5209 DOI: 10.56028/fesr.1.3.1

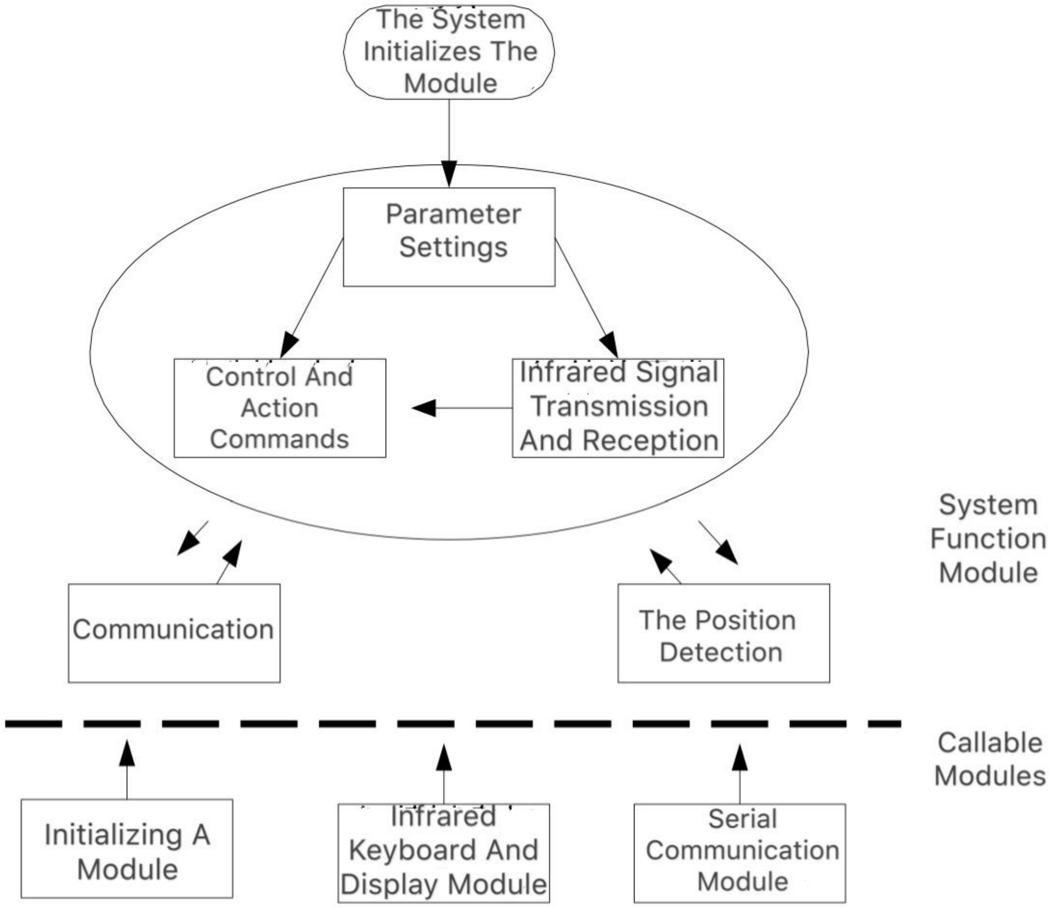


Fig. 2.1 Module relation diagram

ISSN: 2790-5209 DOI: 10.56028/fesr.1.3.1

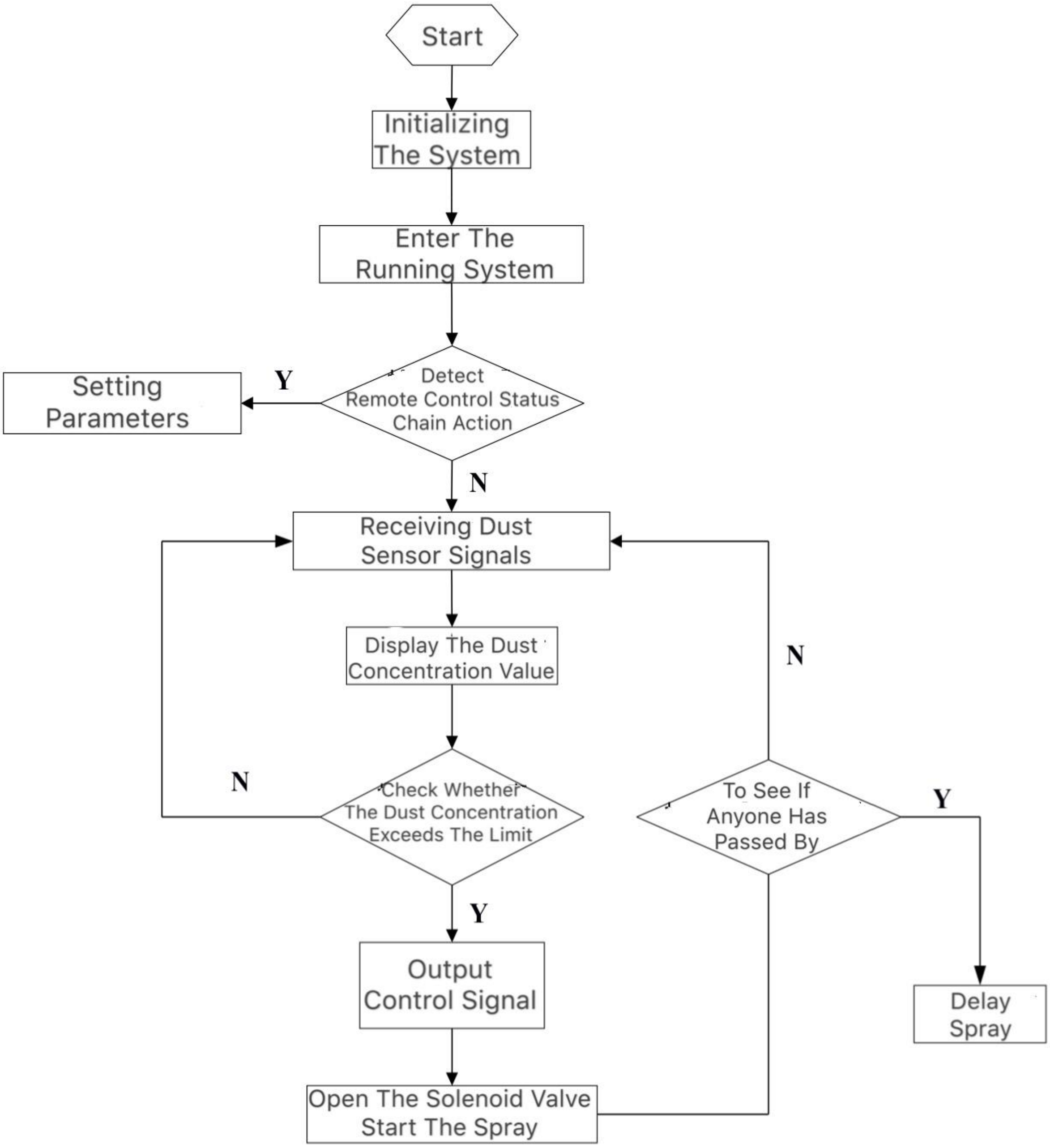


Fig. 2.2 Flow chart of main program

The receiving interrupt program flow is shown in Figure 2.3.

ISSN: 2790-5209 DOI: 10.56028/fesr.1.3.1

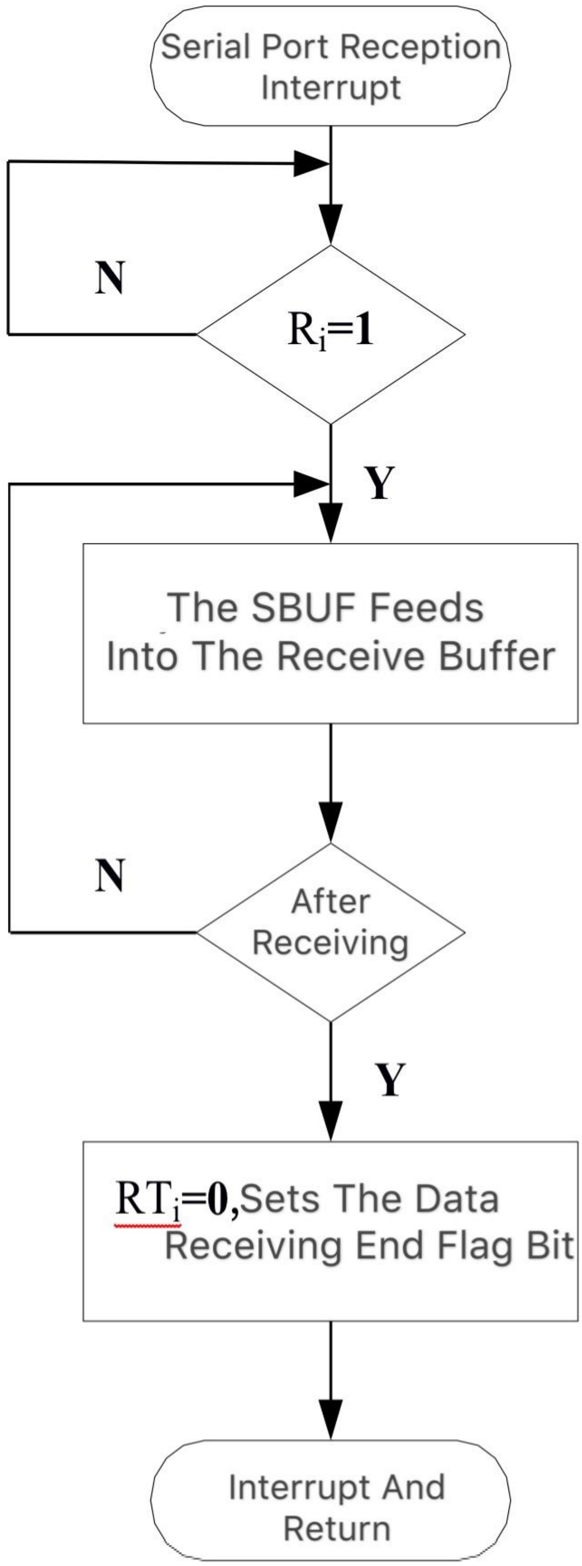


Fig. 2.3 Flow chart of interrupt program

The serial communication program flow is shown in Figure 2.4.

ISSN: 2790-5209 DOI: 10.56028/fesr.1.3.1

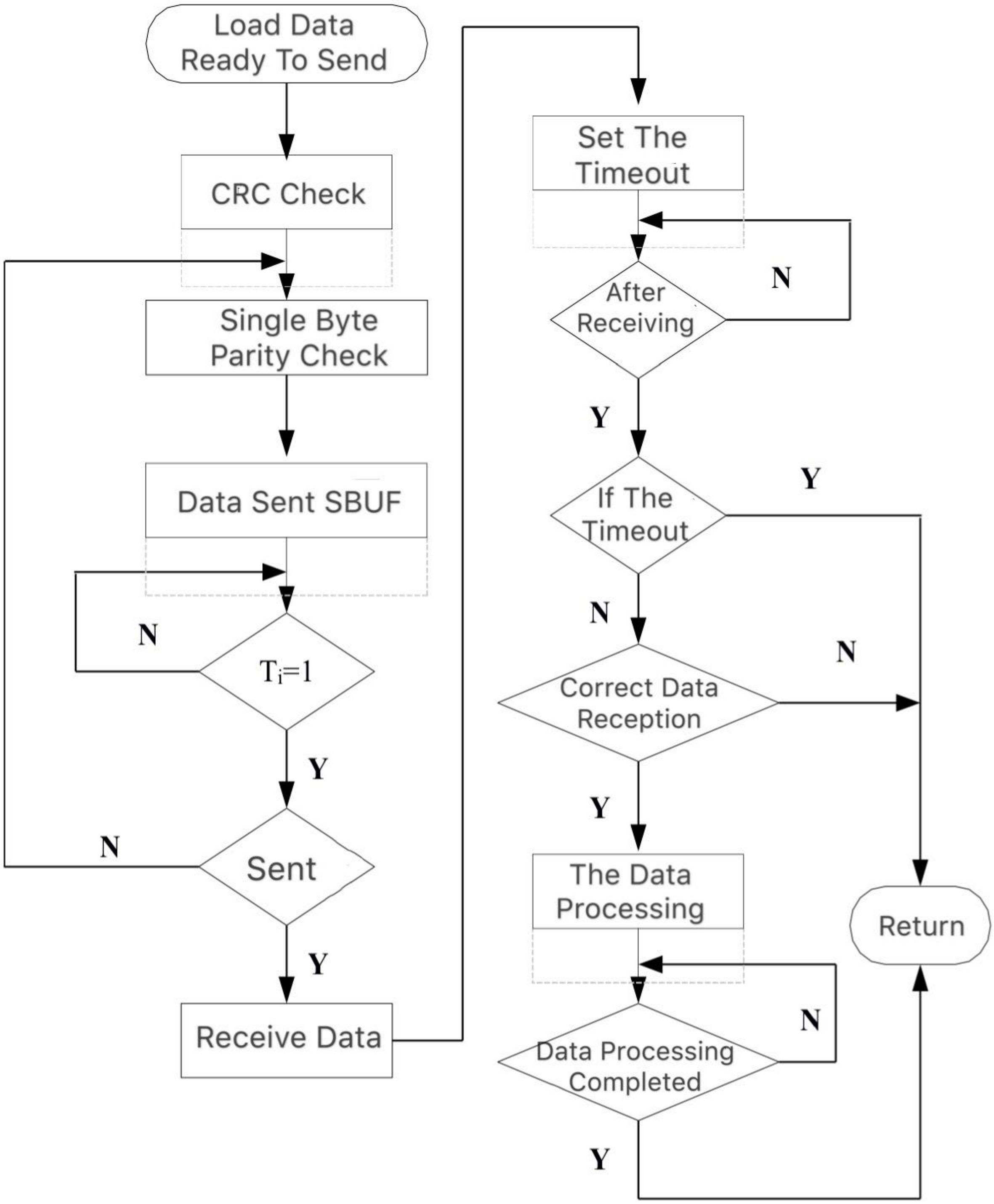


Fig. 2.4 Flow chart of serial communication

# 3. Dust concentration sensor improvement

## 3.1. Improvement scheme of dust concentration sensor

Because of the existing problems of dust concentration sensor, without changing the safety performance of the sensor, the sensors are improved to further improve the accuracy and reliability of the instrument. The specific plan is as follows:

① Increase the automatic calibration function. The RS232 communication circuit is added to

ISSN: 2790-5209 DOI: 10.56028/fesr.1.3.1

the dust meter and sensor, and the concentration coefficient K of the sensor is calibrated by the dust meter through the method of two-machine communication.

② Replace the film pump with a centrifugal fan. According to the technical parameters of the sensor, the technical index of the centrifugal fan is determined, and the size of the impeller, the number of blades, and the type of the vortex housing are determined through theoretical calculation, to design the centrifugal fan suitable for the application of the device.

③ Increase the function of soft starting of centrifugal fan. Because the motor' s direct start will produce a very large impact current, the current is often higher than the power supply current value, thus causing power protection, so that the sensor cannot work normally. This problem can be resolved after the soft start function is added.

④ Increase the watchdog circuit, so that the sensor can maintain normal work in various abnormal situations, which will not happen

The phenomenon of "machine crash".

⑤ Improve the sensor data storage mode, take data and parameters double backup storage measures, and increase the check of CRC code, improve the reliability of data storage.

⑥ Improve the sensor received signal A/D conversion bits, from the original 8-bit A/D to 12-bit A/D, improve the measurement accuracy of the sensor.

⑦ Improved sensor detection algorithm, for the dust concentration size, from the original one-stage detection to multi-stage detection, so that the sensor measurement data is more accurate.

Increase the sensor temperature compensation function to reduce the error caused by the influence of ambient temperature on the photomultiplier tube.

⑨ Added sensor timing automatic correction function, so that the sensor can automatically correct the zero point after running for a certain time.

⑩ Improve the structure of the sensor anachronic chamber, so that the dust air is more smoothly discharged from the instrument, avoid dust pollution photomultiplier tube and laser tube, to improve the service life of the sensor.

By using photomultiplier tubes and HV module seals, the HV module is more adaptable to harsh downhole environments and the sensor is more resistant to dust and moisture.

## 3.2. Specific improvement measures

According to the improvement scheme, the centrifugal fan, start control circuit and temperature compensation circuit involved in the dust concentration sensor are improved. The specific measures are as follows:

① Centrifugal fan design

1) Structure of centrifugal fan

The centrifugal fan is mainly composed of a motor, motor base, fan housing, impeller, connecting pipe and joint, etc. The structure diagram is shown in Figure 3.1.

ISSN: 2790-5209 DOI: 10.56028/fesr.1.3.1

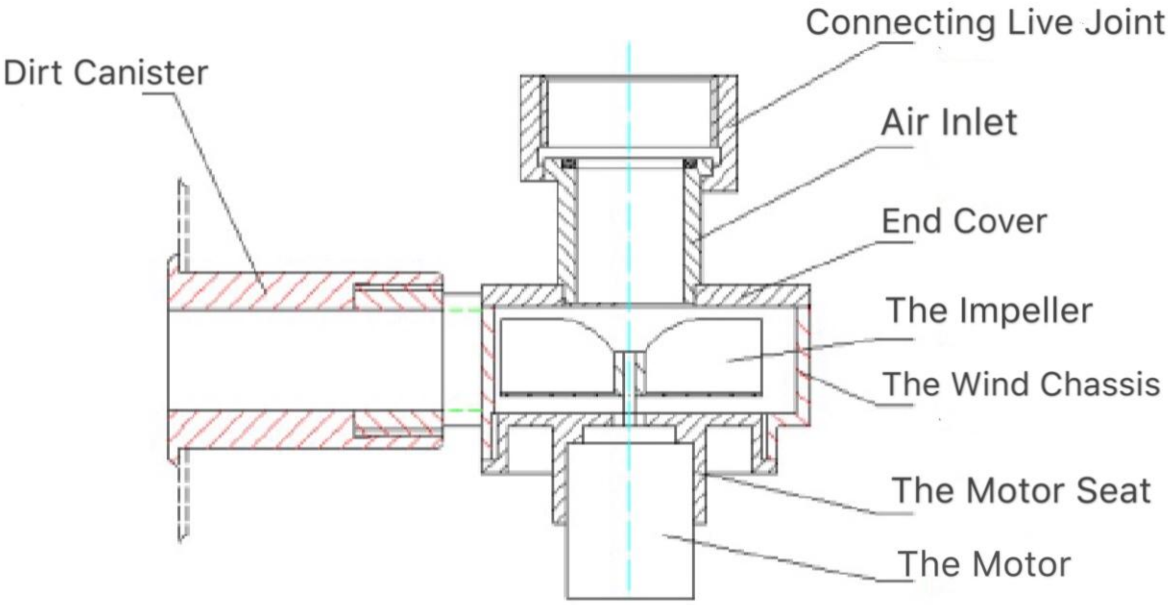


Fig. 3.1 Centrifugal fan structure

2) Design of key components of centrifugal fan

A. Design of impeller

The impeller is the most critical component of the centrifugal fan. Its main function is to increase the static pressure energy and kinetic energy of the gas in the impeller channel through mechanical energy. Considering the use conditions of the fan in the device, the impeller blade and Angle are determined as 90O, and the blade type is selected as a circular blade.

Calculation of impeller outer edge diameter D2:

$$D_2 = \frac{60\omega}{\pi n^2} \quad (4.1)$$

ISSN: 2790-5209 DOI: 10.56028/fesr.1.3.1

Where: $\omega_2$ -- circumferential velocity of impeller, m/s;

n -- motor speed, r/min.

According to formula (1), $D_2$ =49mm.

Calculation of impeller inlet diameter $D_0$:

$$D_0 = \sqrt{\frac{4q_v}{\pi c_0} + d^2} \tag{4.2}$$

Where: $q_v$ -- volumetric flow, $m^3$ /s.

d -- axle diameter, m.

$C_0$ -- impeller inlet speed, m/s (refer to table for selection).

$D_0$ = 5.5 mm.

Leaf inlet diameter $D_1 = 1.1D_0$ =6mm. Determination of the number of leaves:

$$Z = 7.5\frac{\sin \beta_{2A}}{1 - \frac{D_1}{D_2}} \tag{4.3}$$

According to formula (3), the number of leaves Z=8 was determined.

B. volute design

The centrifugal fan uses unequal difference elements to determine the drawing radius of volute.

C. Calculation of motor power P

$$P = K\frac{\left[OP_{sf} + \rho\frac{C_d^2}{2}\right]q_v}{1000\eta_{in}\eta_{me}} \tag{4.4}$$

Where: δ -- compressibility coefficient, δ = 0.9.

K -- design coefficient, K = 1.15.

$P_{sf}$ -- fan static pressure, $P_a$;

$\rho$ -- air density, $\rho$ =1.16kg/ $m^3$;

$C_d$ -- fan outlet air volume, m/s.

$q_v$ -- design flow, $m^3$ /s.

$\eta_{in}$ -- internal efficiency, $\eta_{in}$ = 0.82.

ISSN: 2790-5209 DOI: 10.56028/fesr.1.3.1

$\eta_{me}$ -- mechanical efficiency, $\eta_{me}$ = 0.9. After calculation, the power of fan motor is selected as 0.4W.

②Design of dust concentration sensor fan start control circuit

Considering that the motor in the sensor will produce a very large current directly started, and higher than the power supply current value, resulting in power protection, so that the sensor cannot work normally, using the soft start function, can solve the problem. Paper through the digital potentiometer AD8400 to control the start of the motor, the single chip microcomputer will send signals to the digital potentiometer, control the position of the sliding end of the potentiometer, to change the voltage at both ends of the motor, achieve the soft starts of the motor, to ensure that will not produce large current, from the sensor can operate normally. The fan start control circuit is shown in Figure 3.2.

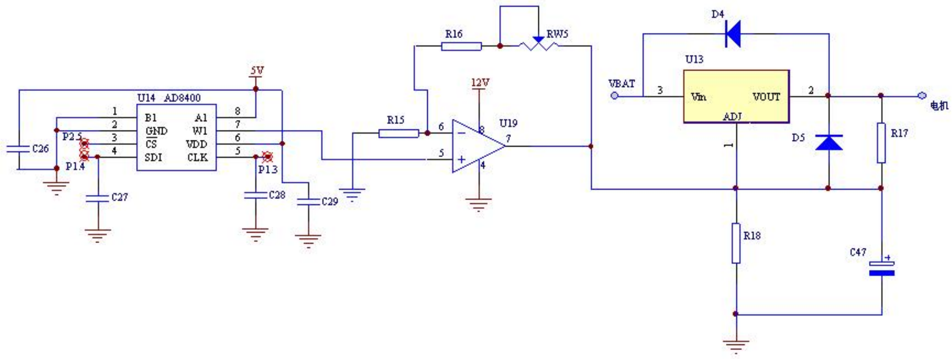


Fig. 3.2 Starting control circuit of generator sensor

③ Design of temperature compensation circuit for dust concentration sensor

Because the output of the photomultiplier tube, the key signal acquisition component in the sensor, will change with the temperature change, the method of temperature compensation is adopted to make up for the loss of output signal. After many tests show that the output of the photomultiplier tube decreases by 0.005V every time the temperature increases by 1℃, and the corresponding dust concentration value is 2mg/m3. According to the algorithm, the compensation calculation in the program can make the measured dust concentration more accurate.

The temperature of the photomultiplier tube is measured by the DS18B20 digital temperature sensor, which can measure the temperature range from -55 ℃ to +125 ℃ . When the temperature is from -10 ℃ to +85℃, the measurement accuracy can reach ±0.5℃.

DS18B20 only needs a port line that can achieve bidirectional communication with the microprocessor and good performance.

④ Improvement of control software

The software design of the sensor is optimized from the aspects of operability, intuitiveness, reliability, and data processing. The watchdog circuit is added to the software to enhance the anti-interference ability and automatic recovery ability of the software. At the same time, the double backup mode is adopted for important data to ensure stability and reliability of the data. The sensor flow is shown in Figure 3.3.

ISSN: 2790-5209 DOI: 10.56028/fesr.1.3.1

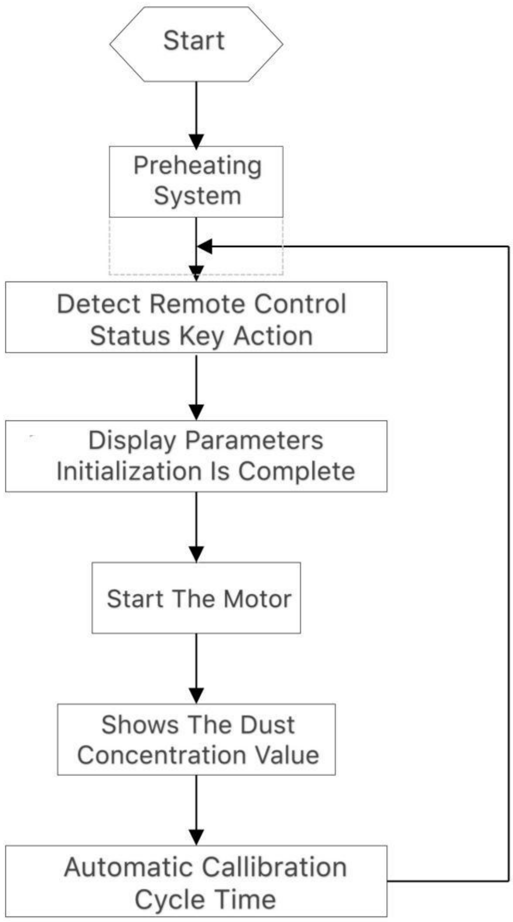


Fig. 3.3 Flow chart of sensor program

⑤ Improvement of circuit and structure of other parts of dust concentration sensor

On this basis, the watchdog circuit is added to the sensor, the data storage method and data algorithm are improved, and the anechoic chamber and chassis structure of the sensor is improved. Increase the watchdog circuit, so that the instrument can maintain normal work in all kinds of abnormal conditions and will not occur a "crash" phenomenon. The method of sensor data storage is improved, and a double backup of data and parameters is adopted. At the same time, the check of CRC code is added, which improves the reliability of data storage. Increasing the number of bits of A/D conversion from the original 8-bit A/D to 12-bit A/D improves the measurement accuracy of the instrument. The detection algorithm of the instrument is improved. According to the concentration of dust, the original one-stage detection is changed to multi-stage detection to make the data measured by the instrument more accurate. The STRUCTURE OF THE ANACHROID CHAMBER IS improved so that the dust air is removed from the instrument more smoothly and the dust pollution to the photomultiplier tube is reduced, and the service life of the instrument is increased. To strengthen the sealing of the sensor case, further measures are taken to seal the photomultiplier tube and high-pressure module, so that the high-pressure module can be more competent for the harsh underground environment and improve the ability of the instrument to prevent dust and moisture.

⑥ Dust concentration sensor performance test

1) Test system

The dust concentration sensor performance test system is shown in Figure 3.4.

ISSN: 2790-5209 DOI: 10.56028/fesr.1.3.1

Under the action of the air pump flow, the dust generator will be sent into the wind tunnel, traction dust generator stepper motor to control the amount of dust, stepping motor speed is controlled by the controller, the dust concentration in the wind tunnel is controlled by the controller, dust meter through the test hole to measure the dust concentration. The wind speed in the wind tunnel is controlled by the variable frequency governor of the fan, and the wind speed range is controlled from 0 to 5m/s.

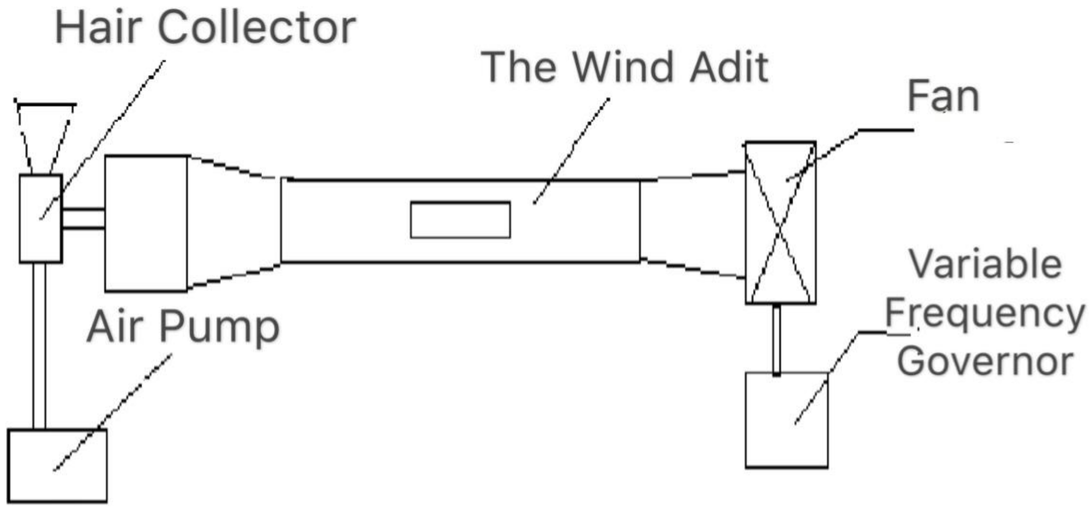


Fig. 3.4 Test system of dust density

2) Test methods and data records

Put two sampling tubes through the parallel test hole in the wind in the edit, a connection dust concentration sensor, another connection dust sampler, the open fan began after dust, dust concentration, since the childhood, record the same period of the dust concentration of dust sampler measurement and sensor dust concentration determination of average contrast calculation.

The dust used in the test was homemade pulverized coal, with a median diameter of 17μm and a true density of 1.5 mg/m3. The test results of particle size distribution are shown in Table 3.5.

Table 4.1 Dust size distribution under testing

| Particle size（μm） | 150 | 100 | 80 | 60 | 50 | 40 | 30 | 20 | 10 | 8 | 6 | 5 |
|---|---|---|---|---|---|---|---|---|---|---|---|---|
| 1 | 0 | 0 | 0 | 0 | 17.3 | 20.4 | 30.4 | 41.5 | 64.6 | 68.4 | 79.0 | 84.5 |
| 2 | 0 | 0 | 0 | 5.8 | 17.0 | 17.0 | 30.7 | 43.8 | 68.9 | 69.4 | 79.4 | 85.4 |
| On average | 0 | 0 | 0 | 2.9 | 17.2 | 18.7 | 30.6 | 42.7 | 66.8 | 68.9 | 79.4 | 85.0 |

Before the test, the dust should be dried for 2 hours and cooled to room temperature before it can be used. Test the wind

The dust concentration in the chamber is measured by the weighing method of filter membrane balance. The calculation formula is as follows:

$$C = \frac{m_2 - m_1}{Qt} \times 1000 \tag{3.5}$$

ISSN: 2790-5209 DOI: 10.56028/fesr.1.3.1

Where: C -- dust concentration, mg/ $m^3$ ;

$m_1$ -- mass of blank filter membrane before sampling, mg.

$m_2$ -- mass of the filter membrane after sampling, mg.

Q -- sampling flow, L/min.

T -- Sampling time, min.

When sampling the filter membrane, 30 groups of data were recorded, and the arithmetic mean value was used as the measurement data. There are three sets of experimental prototypes, numbered 1#, 2# and 3# respectively. The test results are shown in Table 2-2.2 respectively.

Calculation formula of measurement error:

$$\delta = \frac{C_i - C_b}{C_{\max}} \times 100 \tag{3.6}$$

Where: $\delta$ -- measurement error, %.

$C_i$ -- data measured by dust concentration sensor, mg/m.

$C_b$ -- the corresponding point data measured by filter membrane weighing method, mg/m.

$C_{ma}$ -- maximum value measured by filtration membrane weighing method, mg/m.

ISSN: 2790-5209 DOI: 10.56028/fesr.1.3.1

Table 2 .1.1# test results

| The serial number | Weight before sampling (mg) | Weight before sampling (mg) | Filter weight gain (mg) | Sampling time (min) | Dust concentration ($mg/m^3$) | Dust concentration ($mg/m^3$) | Error (%) |
|---|---|---|---|---|---|---|---|
| 1 | 92.7 | 93.6 | 0.9 | | | | |
| 2 | 92.9 | 93.8 | 0.9 | 5 | 28.3 | 26.4 | -0.61 |
| 3 | 91.8 | 92.6 | 0.8 | | | | |
| 4 | 94.3 | 95.4 | 1.1 | | | | |
| 5 | 93.0 | 94.1 | 1.1 | 3 | 61.1 | 58.4 | -0.86 |
| 6 | 95.4 | 95.6 | 1.1 | | | | |
| 7 | 93.7 | 95.7 | 2.0 | | | | |
| 8 | 93.1 | 95.0 | 1.9 | 3 | 111.1 | 112.5 | +0.45 |
| 9 | 91.6 | 93.7 | 2.1 | | | | |
| 10 | 92.2 | 94.4 | 2.2 | | | | |
| 11 | 92.1 | 94.6 | 2.5 | 2 | 195.8 | 205.8 | +3.14 |
| 12 | 92.7 | 96.8 | 4.1 | | | | |
| 13 | 93.2 | 96.8 | 3.6 | | | | |
| 14 | 92.0 | 95.6 | 3.6 | 1 | 627.8 | 573.7 | -8.62 |

ISSN: 2790-5209 DOI: 10.56028/fesr.1.3.1

Table 2.2.1# test results

| The serial number | Weight before sampling (mg) | Weight before sampling (mg) | Filter weight gain (mg) | Sampling time (min) | Dust concentration (mg/m$^3$) | Dust concentration (mg/m$^3$) | Error (%) |
|---|---|---|---|---|---|---|---|
| 1 | 91.9 | 92.5 | 0.6 | | | | |
| 2 | 91.5 | 92.2 | 0.7 | 3 | 37.04 | 35.49 | -0.41 |
| 3 | 90.9 | 91.6 | 0.7 | | | | |
| 4 | 90.9 | 92.3 | 1.4 | | | | |
| 5 | 91.9 | 93.0 | 1.1 | 3 | 70.4 | 68.58 | -0.48 |
| 6 | 92.0 | 93.3 | 1.3 | | | | |
| 7 | 91.6 | 92.6 | 1.0 | | | | |
| 8 | 91.6 | 92.6 | 1.3 | 2 | 100.0 | 103.9 | +1.02 |
| 9 | 91.7 | 93.0 | 1.3 | | | | |
| 10 | 92.4 | 94.1 | 1.7 | | | | |
| 11 | 93.0 | 94.4 | 1.4 | 2 | 136.1 | 128.09 | -2.10 |
| 12 | 93.4 | 95.2 | 1.8 | | | | |
| 13 | 91.8 | 96.8 | 5.0 | | | | |
| 14 | 91.3 | 95.3 | 4.0 | 2 | 380.6 | 403.03 | +5.57 |
| 15 | 92.6 | 97.3 | 4.1 | | | | |

ISSN: 2790-5209 DOI: 10.56028/fesr.1.3.1

Table 2.3.1# test results

| The serial number | Weight before sampling | Weight before sampling | Filter weight gain (mg) | Sampling time (min) | Dust concentration (mg/m$^3$) | Dust concentration (mg/m$^3$) | Error (%) |
|---|---|---|---|---|---|---|---|
| 1 | 76.4 | 77.3 | 0.9 | 6 | 23.15 | 23.15 | 0 |
| 2 | 74.5 | 75.2 | 0.7 | | | | |
| 3 | 76.3 | 77.2 | 0.9 | | | | |
| 4 | 76.2 | 77.2 | 1.0 | | | | |
| 5 | 75.4 | 76.5 | 1.1 | 3 | 55.6 | 47.14 | - |
| 6 | 77.4 | 78.3 | 0.9 | | | | |
| 7 | 76.6 | 79.1 | 2.5 | 2 | 195.8 | 193.1 | - |
| 8 | 73.9 | 76.1 | 2.2 | | | | |
| 9 | 74.8 | 77.6 | 2.8 | 2 | 212.5 | 205.45 | - |
| 10 | 74.9 | 77.2 | 2.3 | | | | |
| 11 | 73.9 | 77.9 | 4.0 | | | | |
| 12 | 75.3 | 79.7 | 4.4 | 1. | 511.1 | 487.6 | - |
| 13 | 76.2 | 81.6 | 5.4 | | | | |

Through three tests, it can be seen from the test results in Table 2-2.2 that compared with the standard data measured by the sampler, the maximum error of the measured value of the dust concentration sensor is -8.62%, which meets the requirement of the basic error ≤±15% in the industry standard of Dust Concentration Sensor for Coal Mine (MT/T 1102-2009). At the same time, the device can be connected to

The dust concentration in the range of 0~1000mg/m3 is effectively measured to meet the design requirements.

## 4. Improvement of light control sensor

### 4.1. Sensor selection and circuit improvement

By comparing the performance of the current market optical control sensors, it is found that the white light sensor, infrared light sensor, and microwave moving target sensor have frequent mis operation, which makes it difficult to popularize in underground coal mine. Comparatively speaking, pyroelectric sensor has the possibility of popularization.

The pyroelectric infrared probe uses the characteristics of pyroelectric material polarization with temperature change to detect infrared radiation and uses the complementary method of the double sensitive element to suppress temperature change, with high sensitivity, so that it can only sense the infrared band of human radiation, not be interfered by other radiation, and improve the anti-interference performance of the sensor. Its output electrical signal > 2.0V, working temperature -20℃ -60 ℃, the field of view 155°×145°.

Because the output of the pyroelectric probe is weak, the paper designs the signal amplifier circuit and outputs the electrical signal to the main control circuit board of the control module after amplification for modulation, amplification, and delay processing. The designed circuit is

ISSN: 2790-5209 DOI: 10.56028/fesr.1.3.1
shown in Figure 4.11.

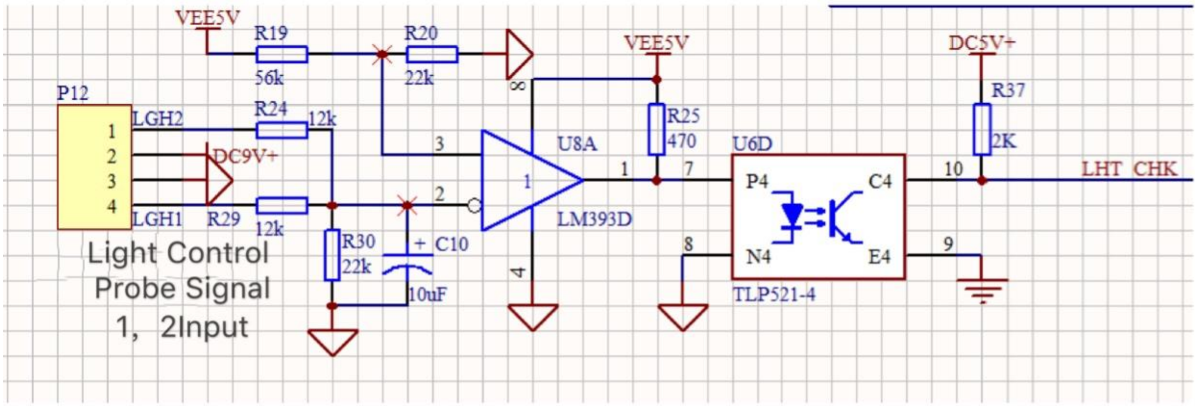

Fig. 4.1 Circuit diagram of light control sensor

## 4.2. Sensor selection and circuit improvement

The test was carried out according to the "CGHRK1 type light control sensor Enterprise Standard" (Q/MKC 171-2003). The light control sensor is a device that senses infrared radiation of the human body and converts it into an electrical signal. The signal system test circuit diagram is shown in Figure 4.2.

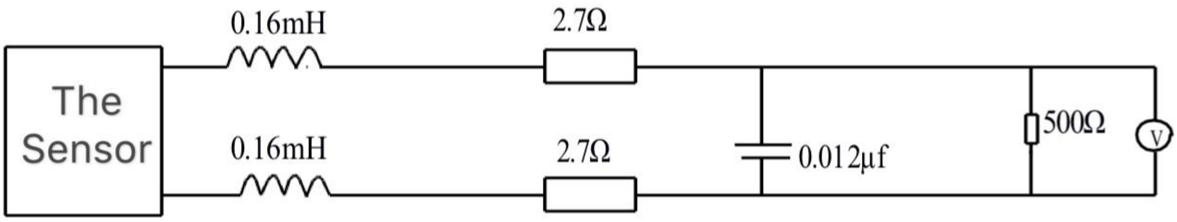

Fig. 4.2 Signal experiment circuit diagram of light control sensor

① Test instrument:

1) DC voltmeter: 0 ~ 15V level 0.2.

2) Tape measure: 0 ~ 15m.

② Test method and data record

Personnel from near too far away from the light sensor probe at different distances to measure the sensor output voltage signal. After repeated measurement, the test results are shown in Table 4.5.

ISSN: 2790-5209 DOI: 10.56028/fesr.1.3.1

Table 4.5 Test results of light control sensor

| Control distance (M) | The sensitivity | Signal output | Voltage signal (V) |
|---|---|---|---|
| 1 | High | High level | 3.5 |
| 2 | High | High level | 3.5 |
| 3 | High | High level | 3.5 |
| 4 | High | High level | 3.5 |
| 5 | High | High level | 3.5 |
| 6 | High | High level | 3.5 |
| 7 | High | High level | 3.5 |
| 7.5 | High | High level | 3.5 |
| 8 | High | High level | 3.5 |
| 8.5 | High | High level | 3.5 |
| 9 | High | High level | 3.5 |
| 9.5 | High | High level | 3.5 |
| 10 | High | High level | 3.5 |
| 10.5 | On the low side | When high low | 3.5/0 |
| 11 | Low | Low level | 0 |

The output signal of the optical control sensor is high and low levels. When it detects someone passing by, it outputs a high level (voltage is 3.5V), and when it cannot be monitored, it outputs a low level (voltage is 0V). The test results show that the effective measuring distance range of the optical control sensor is 0 ~ 10m, which meets the design requirements.